Modification of hypereutectic Al-Si alloy surface layer structure by Nb alloying under high temperature plasma impact

N.N.Cherenda[1,*], N.V.Bibik[1], V.M.Astashynski[2,3], A.M. Kuzmitski[2]

[1]Belarusian State University, Nezavisimosti ave., 4, Minsk 220030, Belarus

[2]A.V. Luikov Heat and Mass Transfer Institute, National Academy of Sciences of Belarus, P. Brovki str., 15, Minsk 220072, Belarus

[3]National Research Nuclear University "MEPhI" (Moscow Engineering Physics Institute), Kashirskoe Ave., 31, Moscow 115409, Russia

* Address all correspondence to: Nikolai Cherenda, Belarusian State University, 4 Nezavisimosty Ave, Minsk 220030, Belarus. E-mail: cherenda@bsu.by, Tel.: +375172095408; Fax: +3752095445

Abstract

Phase composition, microstructure and microhardness of the hypereutectic Al-Si alloy (22.3 wt.% of Si) surface layer alloyed with Nb atoms under compression plasma flows treatment (energy absorbed by the surface layer 25-35 J/cm^2 per pulse) was investigated in this work. X-ray diffraction analysis, scanning electron microscopy were used for surface layer characterization. The findings showed that plasma impact on Nb/Al-Si system led to the alloyed layer formation in Al-Si with the thickness of 10-45 μm that was dependent on the treatment regimes. Alloyed layer contained $(Al,Si)_3Nb$ intermetallic compound. Alloying of Al-Si with niobium atoms led to its hardening. Annealing of alloyed samples at 170 °C in air also resulted in microhardness growth.

Keywords: silumin, niobium, compression plasma flow, phase and element composition, microstructure, microhardness

Introduction

The modern development of technology requires new materials with a complex of high performance characteristics and high manufacturability in the production process. A special place is occupied by alloys with low values of the thermal coefficient of linear expansion in combination with the required level of mechanical properties. Hypereutectic Al-Si alloys belong to this group of materials. The introduction of a large amount of silicon into aluminum (from 20 wt.% and above) provides a low coefficient of linear expansion of the alloy (Laskovnev, et.al., 2013). However, for the practical use of hypereutectic silumin as a structural material, it is necessary to solve a number of problems associated with their unsatisfactory mechanical properties, in particular high fragility (Laskovnev, et.al., 2013; Zolotorevsky, et.al., 2007).

Currently, active research is carried out on the formation of new types of aluminum alloys, including those based on Al-Si system, which have high strength properties and high heat resistance. Formation of composites in which transition metals trialuminides are used as hardening particles is one of the research directions. These intermetallides have a high melting point, low density, high modulus of elasticity, good resistance to oxidation, and low ability to coalescence (Laskovnev, et.al., 2013; Zhang, et.al., 2020; Nong, et.al., 2012; Wang, et.al., 2014). Besides that addition of Zr and Nb as alloying elements has a great structure refining effect (Wang, et.al., 2014; Li, et.al., 2019).

The performance characteristics of materials surface layer can be improved by exposure to electron, ion, plasma and laser beams (Akamatsu, et.al., 2002; Cherenda, et.al., 2020; Vilar, et.al., 1999; Akhmadeev, et.al., 2021; Borowski, et.al., 2010; Konovalov, et.al., 2020; Shymanski, et.al., 2021). The main advantages of such modification methods are structure dispersion (including primary silicon crystals in silumin), synthesis of nanosized metastable phases, as well as nanocomposites and intermetallic compounds with unique physicochemical characteristics (Konovalov, et.al., 2020; Cherenda, et.al., 2014; Zhang, et.al., 2019). The use of such methods for the modification of aluminum alloys is especially relevant, the wider application of which in industry is constrained by low tribological and strength characteristics. Earlier obtained results have shown that treatment of Al-Si alloys by high-intensity electron beams and plasma flows of submillisecond duration led to a significant improvement in wear resistance, fatigue, heat resistance, etc. (Laskovnev, et.al., 2013; Konovalov, et.al., 2020; Cherenda, et.al., 2014; Zaguliaev, et.al., 2021)..

Compression plasma flows (CPF) can be used to alloy the surface layer of materials with additional elements. Alloying is carried out by preliminary deposition of a film or coating containing alloying elements on the surface of the material and subsequent exposure to

plasma flows. High temperature plasma impact leads to melting of the coating and the surface layer of the substrate, liquid-phase mixing of the components in the melt as a result of the occurrence of convective flows. After the end of the pulse, ultrafast cooling of the melt occurs. The combination of two approaches in this method, providing both the alloying of the surface layer and the dispersion of its structure as a result of melt fast quenching, can be a promising method for the formation of surface layers in silumin with improved performance. In particular, it was shown that CPF impact on eutectic silumin coated with Ti, Zr or Nb resulted in the formation of a composite surface layer containing a supersaturated aluminum solid solution and fine intermetallic phases on the basis of Al_3Ti, Al_3Zr, and Al_3Nb compounds respectively with a tetragonal $D0_{22}$ type of crystalline structure (Cherenda, et.al., 2014). The synthesized composite layer possessed a high hardness value (up to 4.4 GPa).

Similar approach - alloying of hypereutectic silumin with Nb atoms under CPF impact - was used in this work to improve mechanical properties of the alloy. Nb was chosen among other transition elements forming trialuminides because Al_3Nb has good oxidation resistance [3, 4] and has the highest melting temperature (1605 ^oC (Lyakishev, 1996)) that may ensure higher mechanical properties at elevated temperatures.

Experimental

Hypereutectic Al-Si alloy (22.3 Si, 0.8 Mg, 0.6 Cu, 0.3Ni, 1.3 Fe, the rest is Al, in at.%) was the investigation object. Niobium coating was formed on the samples by vacuum cathode-arc deposition technique with the following process parameters: arc current 190 A, bias voltage -120 V, deposition time 10 min. Coating thickness was ~ 4 μm. Treatment of Nb coated samples by three plasma pulses was carried out in a gas-discharge magnetoplasma compressor of compact geometry, in which the acceleration of the plasma in an axially symmetric system of two electrodes is accompanied by its compression due to the interaction of the longitudinal component of the current with its own azimuthal magnetic field. The discharge duration was ~ 100 μs. Before the discharge, the pre-evacuated vacuum chamber was filled with a nitrogen up to a pressure of 400 Pa. The density of the energy absorbed by the surface in one pulse (Q) was changed in the range of 25-35 J/cm^2 by varying the distance between the cathode and the sample. The phase composition was studied by X-ray diffraction analysis using a RIGAKU Ultima IV diffractometer in the geometry of a parallel beam in Cu Kα radiation. Samples cross-section morphology was studied using scanning electron microscopy on a LEO1455VP microscope. The elemental composition of the samples was determined by X-ray spectral microanalysis using an Oxford Instruments detector coupled to a scanning electron

microscope. Vickers microhardness of the samples was measured on a PMT-3 device with a load on the indenter of 0.5-2 N.

Results and discussion

The impact of the CPF on the Nb / Al-Si system led to melting of the coating and the surface layer of the substrate, their liquid-phase mixing and subsequent fast cooling (up to 10^7 K/s (Laskovnev, et.al., 2013)). Surface layer of silumin doped with niobium atoms was formed as a result. Figure 1 shows the cross-section morphology of the Nb/Al-Si system samples after CPF impact with different energy density absorbed by the surface and the distribution of elements along the cross-section depth. Plasma impact resulted in dissolution of intermetallides existed in the initial alloy surface layer. In particular, in Figures 1a – 1d one can see Al-Fe-Si particles which elemental composition is close to composition of βAl_5FeSi phase already observed in Al-Si alloys. Plasma impact led to dissolution of precipitate part appeared in the melt and precipitate cracking. The last effect was also observed after submillisecond electron beam treatment of Al-10Si-2Cu alloy (Konovalov, et.al., 2020). Change of the treatment parameters significantly affected the thickness of the alloyed layer. The alloyed layer thickness was increased from 10-30 μm (at Q = 25 J/cm^2) to 40-45 μm (at Q = 35 J/cm^2). The alloyed layer also contained spherical pores which size can be varied from 0.3-2 μm (Figure 1a) up 10 μm (Figure 1c). Increase of the energy absorbed by the surface layer led to pores disappearance (Figure 1e).

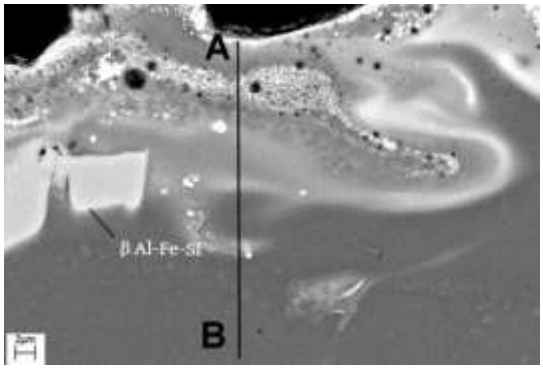

a

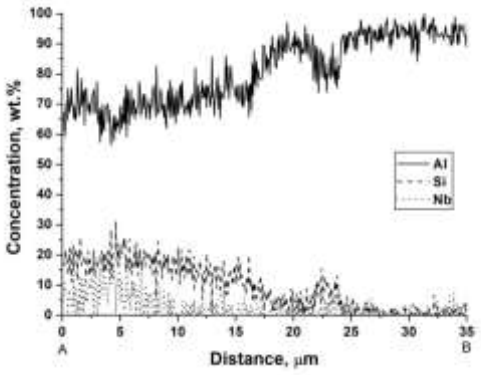

b

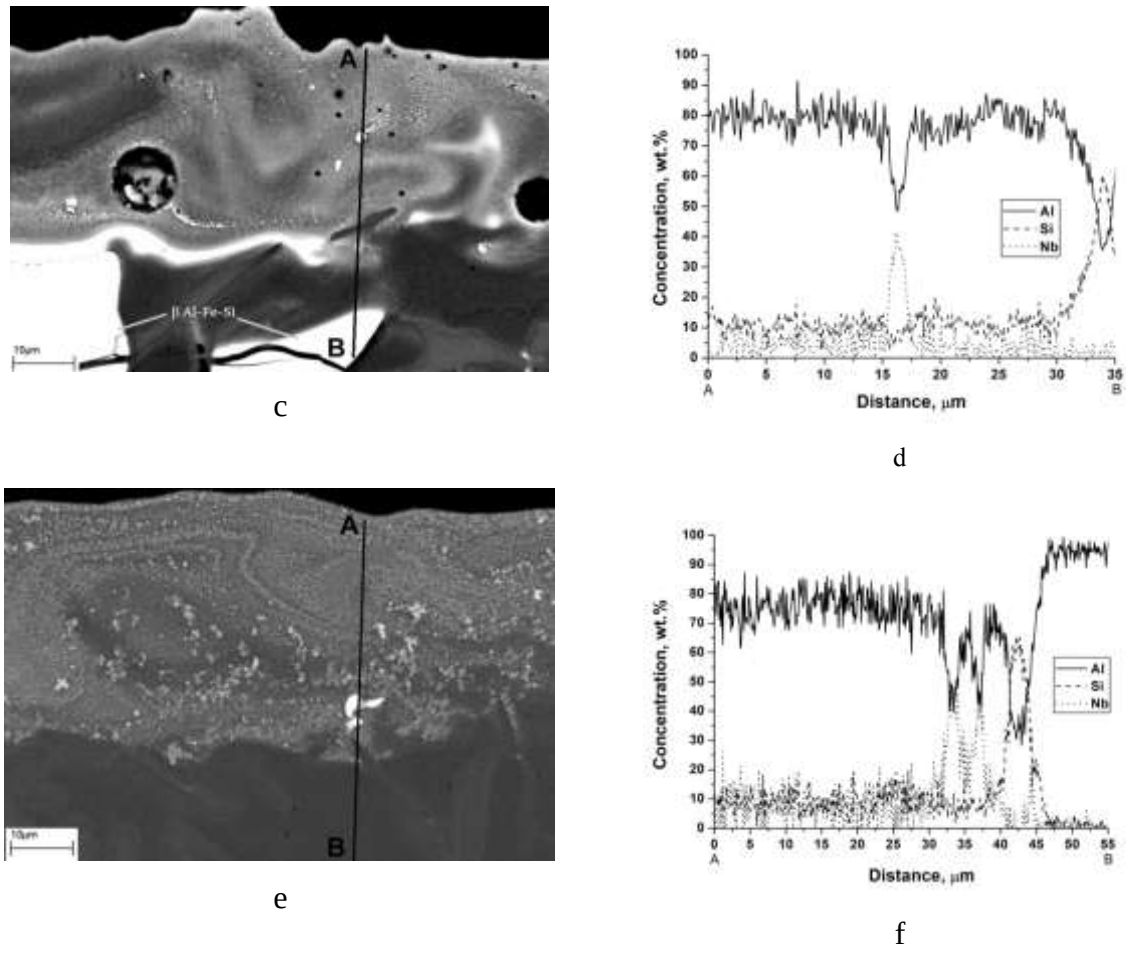

Figure 1. Cross-section morphology (a, c, e) of the samples treated by CPF at different energy absorbed by the surface and distribution of elements along the depth (b, d, f): Q=25 J/cm^2 (a, b), Q=30 J/cm^2 (c, d), Q=35 J/cm^2 (e, f).

Besides that the alloyed layer was characterized by a more uniform distribution of the alloying element along the depth with the growth of the energy density. This effect can be explained by the increase of the melt lifetime and greater duration of convection processes action in the melt leading to melt elemental composition homogenization. At the same time even after plasma treatment at the maximum absorbed energy density (Q=35 J/cm^2) inclusions of undissolved niobium were observed in the depth of the alloyed layer (Figures 1e, 1f) due to the significant difference in the melting temperatures of niobium and Al-Si eutectics. The concentration of niobium in the area with uniform distribution was about 10 wt. %. The alloyed layer of the samples contains dendritic shaped niobium-containing precipitates with the size of as small as 200 nm (Figure 2). A similar shape of precipitates was observed for $(Al, Si)_3Ti$ and $(Al,Si)_3Zr$ phases with $D0_{22}$ crystalline structure (Cherenda, et.al., 2014; Srinivasan, et.al., 2001). X-ray microanalysis give information on average concentration of

elements in the area with lateral resolution ~ 1 μm. That is why it is impossible to determine accurate composition of Nb containing precipitates showed in Figure 2.

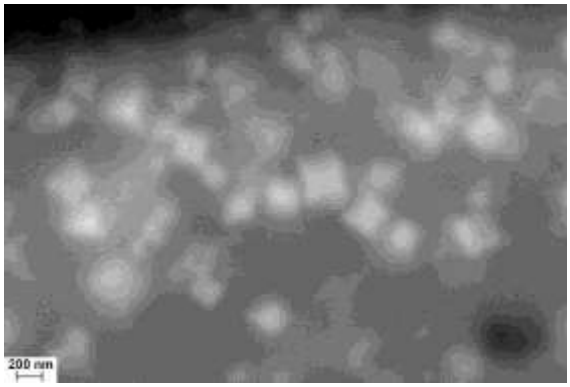

Figure 2. Cross-section morphology of the sample treated by CPF at Q=35 J/cm^2.

At the same time such an attempt can be made in the areas of non uniform mixing of coating and substrate material. In Figure 3a one can see the formation of dendrites growing from undissolved Nb particles into the alloy matrix. The transition area between Nb particle and Al-Si matrix that contained dendrites corresponded to almost constant distribution of elements that can indicate formation of compound (Figure 3b). The average concentration of Al was 61 at.% ,Nb ~ 26 at.% and Si ~ 13 at.% in this area. The elements ration corresponded well to composition of $(Al,Si)_3Nb$ compound. It should be noted that Si concentration in this compound was much less than it concentration in the alloy. So one can conclude that the value of ~ 13 at.% was the maximum Si concentration in the solid solution on the basis of Al_3Nb. This value is close to that of (10 at.%) received in (Liu, et.al., 2017) for $(Al,Si)_3Zr$ compound.

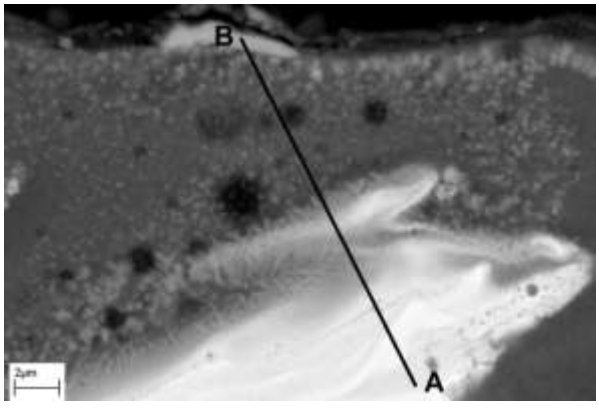

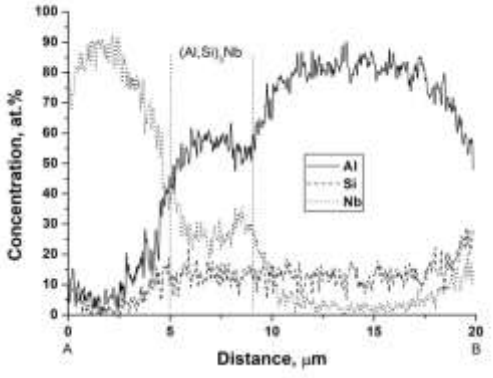

a) b)

Figure 3. Cross-section morphology (a) of the sample treated by CPF at Q=30 J/cm^{2}and distribution of elements along the line A-B (b)

Figure 4 shows the diffraction pattern of the Al-Si samples before and after Nb deposition. Al, Si and β-Al_5FeSi phases were found in the structure of initial sample. The intensity of Si and β-Al_5FeSi diffraction lines was significantly diminished after coating deposition due to strong X-ray absorbance by Nb. CPF impact led to significant diminishing of Nb diffraction lines intensity and disappearance of β-Al_5FeSi diffraction lines (Figure 5) that correlated with the data of cross-section analysis (Figure 1). Formation of the intermetallic compound on the basis of Al_3Nb was found in the surface layer (Figure 5). Al_3Nb formation with tetragonal crystalline lattice was already observed in (Vilar, et.al., 1999) after laser processing of Al-Nb coatings.

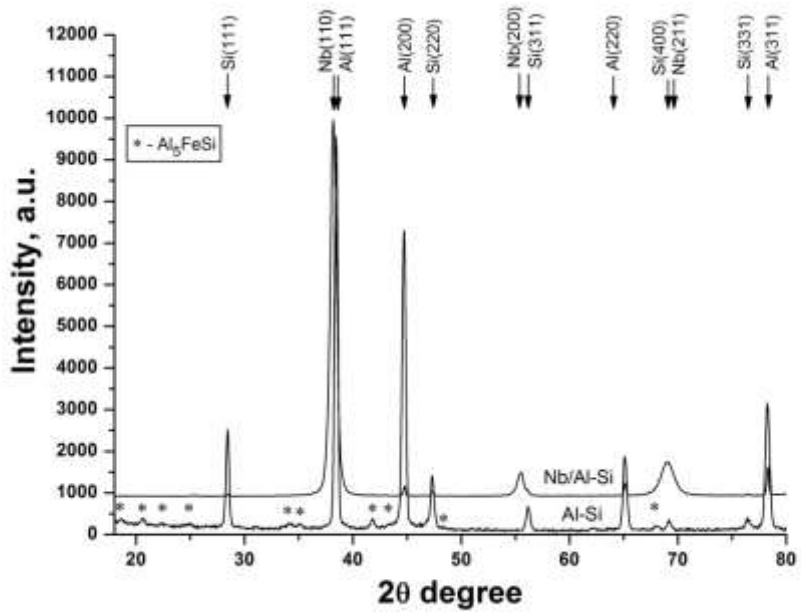

Figure 4. Diffraction patterns of Al-Si samples before and after Nb coating deposition.

The diffraction lines of the Al_3Nb intermetallic compound were shifted relative to the standard to the region of higher diffraction angles, that could be caused by the inclusion of silicon atoms into the crystalline lattice of the intermetallic compound and the formation of a substitutional solid solution $(Al,Si)_3Nb$. The lattice parameter *a* of $(Al,Si)_3Nb$ phase formed in the sample treated at Q=30 J/cm^2 was 0,5406 nm, while the lattice parameter *a* of the Al_3Nb standard - 0,5427nm. At the same time the lattice parameter *c* of the $(Al,Si)_3Nb$ phase (0,8589 nm) was close to that of the standard (0,8584nm). Formation of substitutional solid solution based on trialuminides was already observed in Al-Si-Ti and Al-Si-Zr systems (Cherenda, et.al., 2014; Tong, et.al., 2012). The results obtained allow making a conclusion that niobium-

containing inclusions detected by electron microscopy in Figures 2 and 3 could be attributed to $(Al,Si)_3Nb$ intermetallic compound.

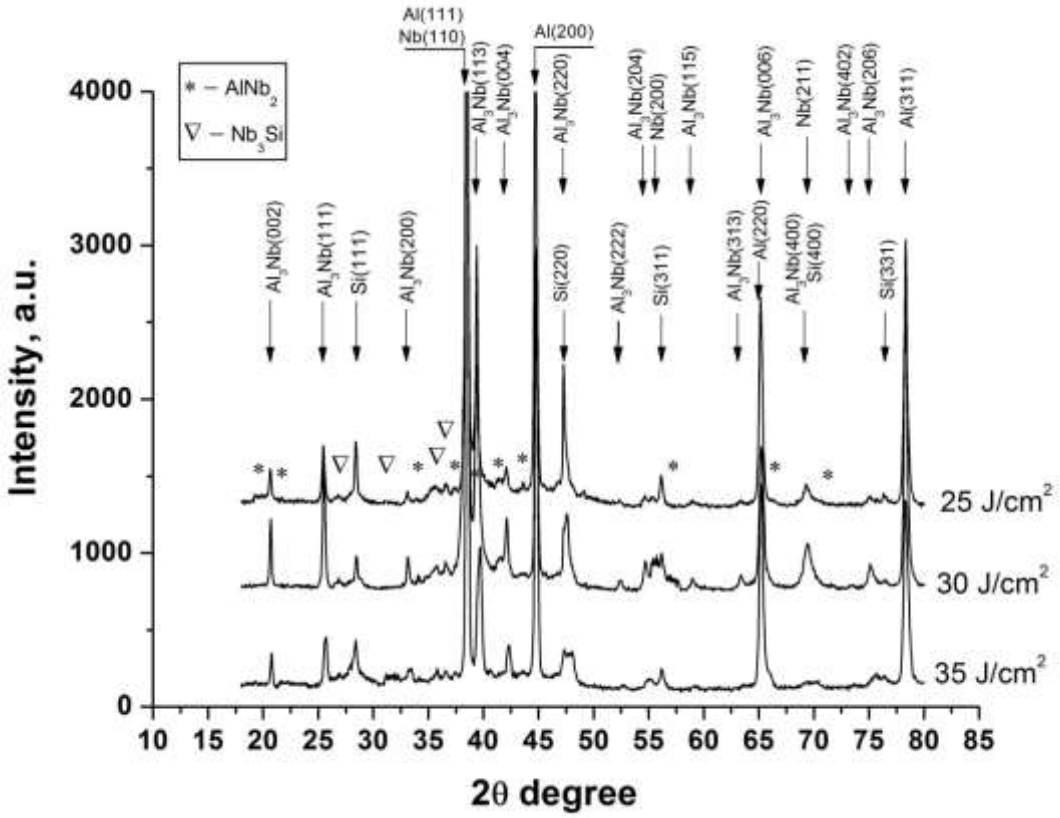

Figure 5. Diffraction patterns of samples treated by CPF at different energy absorbed by the surface.

Comparing the obtained diffraction patterns, one can note a nonmonotonic dependence of $(Al,Si)_3Nb$ lines intensity, which is proportional to the volume fraction of the intermetallic compound in the alloyed layer, on the absorbed energy density. The maximum of intermetallic compound volume fraction was observed at Q=30 J/ cm^2. A possible reason for this behavior was the competition between the two processes. Increase of the energy absorbed by the surface layer should led to diminishing of alloying element concentration in the surface layer due to the growth of the melt layer thickness and increase of surface erosion intensity (Laskovnev, et.al., 2013). Thus a decrease in the volume fraction of intermetallic compounds should occur. On the other hand, samples treatment at a low density of Q could lead to the formation of only local areas of mixing (Laskovnev, et.al., 2013). An increase in the absorbed energy density caused melting of the entire surface layer and a more uniform mixing of the coating and substrate components, due to which the volume fraction of intermetallic compounds should increase.

Weak diffraction lines of the intermetallic compound based on $AlNb_2$ with tetragonal crystalline structure were also observed in diffraction patterns of CPF treated samples. The latter phase could be formed in local regions enriched in niobium due to inhomogeneous mixing, in particular, in the areas between undissolved Nb particles and areas corresponding to $(Al,Si)_3Nb$ (Figure 3).

The diffraction patterns in figure 5 also contained diffraction lines of Nb_3Si, NbN and Nb_2N phases with low intensity. It should be noted that silicide phase was not found by scanning electron microscopy. This is may be related to low content of Nb_3Si phase in the alloyed layer and small dimensions of it precipitates. In contrast to the results obtained in this work in (Tong, et.al., 2012) it was shown that silicide, in particular $Zr(Al,Si)_2$, should be predominant phase instead of $(Al,Si)_3Zr$ intermetallide in case of Zr addition into hypereutectoid Al-Si alloys. In these experiments Nb formed mainly intermetallides in the alloyed layer. NbN and Nb_2N nitrides were formed at the surface of the samples due to the interaction of niobium atoms with nitrogen atoms of the residual atmosphere of the vacuum chamber. Formation of niobium nitrides was also observed in (Cherenda, et.al., 2018) after CPF treatment of NbC/AISI T1 steel system by CPF.

X-ray diffraction data showed a broadening and a decrease in the intensity of the silicon diffraction lines after CPF treatment. This effect was observed due to the formation of dispersed silicon precipitates crystallizing from the melt under ultrafast cooling conditions. In addition, some silicon atoms participated in the formation of solid solution based on intermetallic compounds.

Rapid cooling of the surface layer from the melt determined its metastable structure. Annealing was carried out to test phase composition and mechanical properties stability under elevated temperature. Silumin sample treated with three CPF pulses at Q=35 J/cm^2 was annealed in air for 1-3 hours at a temperature of 170 °C (~ 0.3 of the Al-Si eutectic temperature in order to avoid recrystallization processes). No phase composition changes were revealed after annealing. At the same time the following effect was found (Figure 6). One can see from the figure that shift of $(Al,Si)_3Nb$ diffraction lines positions towards to the positions of the standard diffraction lines (marked as Al_3Nb in the Figure 6) took place. So the gap between closely located Si and $(Al,Si)_3Nb$ diffraction lines disappeared after 1 hour of annealing. A possible reason for this effect is the precipitation of Si particles from $(Al,Si)_3Nb$ solid solution leading to intermetallide lattice parameter increase.

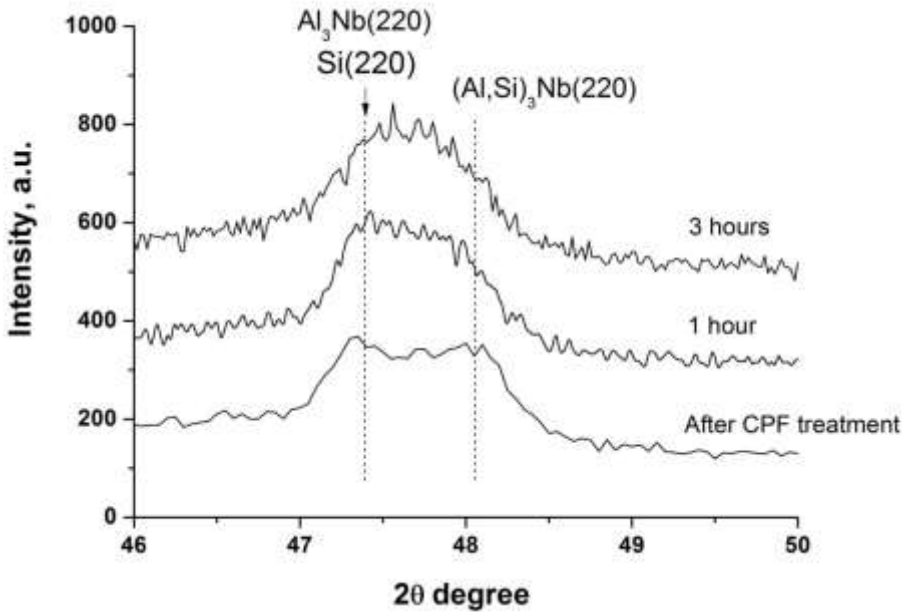

Figure 6. Part of diffraction patterns of sample treated by CPF at Q=35 J/cm^2 and annealed at 1 and 3 hours.

Figure 7 shows the dependences of the microhardness values on the indenter penetration depth of silumin samples treated by CPF. One can see that increase of the energy absorbed by the surface layer led to diminishing of the microhardness. At the same time it should be noted that microhardness changes occured almost within the measurement error due to the developed surface morphology. However, the microhardness of the alloyed samples in the near-surface layer was somewhat higher than that of the initial one. Thus one could make a conclusion that alloying of silumin with niobium atoms led to its hardening. An increase in microhardness could be associated with both the formation of intermetallic precipitates and the formation of niobium nitrides. Annealing led to microhardness increase (Figure 8). This effect could be explained by the appearance of dispersed Si precipitates due to release of Si from the supersaturated solid solution $(Al,Si)_3Nb$.

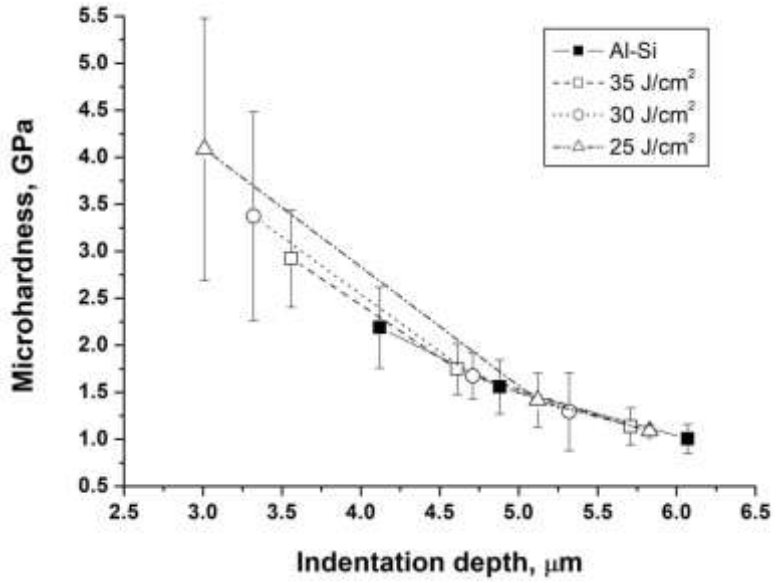

Figure 7. Dependences of the microhardness on the indenter penetration depth of initial silumin sample and samples treated by CPF.

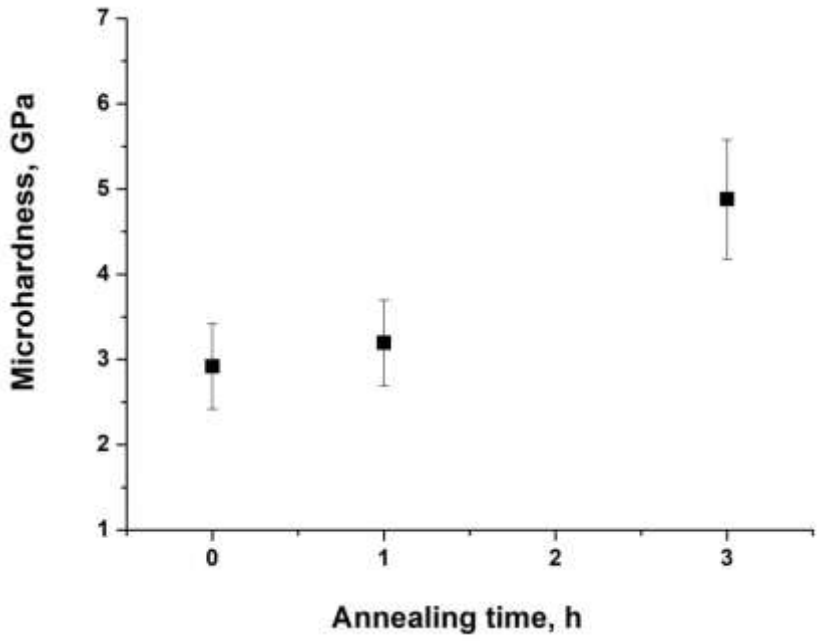

Figure 8 Dependence of the microhardness on the annealing time of sample treated by CPF at Q=35 J/cm^2.

Conclusions.

It was found that compression plasma flow impact (the energy density absorbed by the sample surface was 25-35 J/cm^2 per pulse) on the Nb / Al-Si system led to silumin surface layer alloying with niobium atoms. An increase in the energy density absorbed by the surface layer

resulted in growth of niobium distribution uniformity. Formation of disperse $(Al,Si)_3Nb$ precipitates as small as ~ 200 nm was found in the alloyed layer. Interaction of niobium atoms with nitrogen atoms of the residual atmosphere of the vacuum chamber resulted in niobium nitrides synthesis. A change in the absorbed energy density led to a nonmonotonic dependence of $(Al,Si)_3Nb$ volume fraction in the analyzed layer. A broadening of the silicon diffraction lines was observed on the diffraction patterns after CPF treatment that was associated with the formation of dispersed primary silicon crystals crystallized from the melt. Alloying of silumin with niobium atoms led to surface layer hardening. Annealing of alloyed samples at 170 °C in air also resulted in microhardness growth.

References.

Akhmadeev, Y. H., Ivanov, Y. F., Krysina, O.V., Lopatin, I. V., Petrikova, E. A., Rygina, M.E., Electron-ion-plasma modification of carbon steel, *High Temperature Material Processes*, Vol. **25**, no. 1, pp. 47-55, 2021.

Akamatsu, H., Tanaka, Y., Yamanishi, T., Egawa, S., Yamasaki, T., Miki, M., Yatsuzuka, M., Increase of Si solution rate into Al matrix by repeated irradiation of intense pulsed ion beam, *Vacuum*, Vol. **65**, p. 563-569, 2002.

Borowski, J., Bartkowiak, K., Investigation of the influence of laser treatment parameters on the properties of the surface layer of aluminum alloys, *Physics Procedia*, Vol. **5**, 449–456, 2010.

Cherenda, N. N., Bibik, N. V., Uglov, V. V., Astashynski, V. M., Kuzmitski, A. M., Synthesis of surface layers hardened by metal trialuminide compound in Al–Si alloy under compression plasma flows impact, *High Temperature Material Processes*, Vol. **18**, no 1–2, pp. 1–13, 2014.

Cherenda, N.N., Uglov, V.V., Kashevski, A.M., Astashynski, V.M., Kuzmitski, A.M., Remnev, G.E., Combined plasma and thermal treatment of the NbC/AISI T1 steel system, *High Temperature Material Processes*, Vol. **22**, no. 1, pp. 1–11, 2018.

Cherenda, N.N., Uglov, V.V., Martinovich, Yu.V., Betanov, I.A., Astashynski, V.M., Kuzmitski, A.M., Structure of the austenitic steel surface layer subjected to compression plasma flows impact, *High Temperature Material Processes*, Vol. **24**, no. 3, pp. 211–225, 2020.

Konovalov, S., Zaguliaev, D., Ivanov, Y., Gromov, V., Abaturova, A., Modification of Al-10Si-2Cu alloy surface by intensive pulsed electron beam, *Journal of Materials Research and Technology*, Vol. **9**, no. 3, pp. 5591–5598, 2020.

Laskovnev, A. P., Ivanov, Yu F., Petrikova, E. A., Koval, N.N., Uglov, V.V., Cherenda, N.N., Bibik, N.V., *Modification of structure and properties of eutectic silumin by electron-ion-plasma treatment*. Minsk: Belarusskaya Nauka, 2013. (in Russian)

Li, Y., Hu, B., Gu, Q., Liu, B., Li, Q., Achievement in grain-refining hypoeutectic Al-Si alloys with Nb, *Scripta Materialia*, Vol. **160**, pp. 75–80, 2019.

Liu, Y., Tang, M., Wu, C., Wang, J., Su, X., Progress on phase equilibria of the Al-Si-Zr system at 700 and 900^{o}C, *Journal of Alloys and Compounds*, Vol. **693**, pp. 357-365, 2017.

Lyakishev, N.P., Ed., *Phase Diagrams of Binary Metal Systems: Handbook*, vol. **1**, Moscow, Russia: Mashinostroenie Press, 1996. (in Russian)

Nong, Z., Zhu, J., Yang, X., Cao, Y., Lai, Z., Liu, Y., The mechanical, thermodynamic and electronic properties of Al_3Nb with D022 structure: A first-principles study, *Physica B*, vol. **407**, pp. 3555–3560, 2012.

Srinivasan, D., Chatoopadhyay, K., Metastable phase evolution and hardness of nanocrystalline Al–Si–Zr alloys, *Mater. Sci. Eng.*, Vol. **A304–306**, pp. 534–539, 2001.

Shymanski, V. I., Jevdokimovs, A., Cherenda, N. N., Astashynski, V. M., & Petrikova, E. A., Structure and phase composition of hypereutectic silumin alloy Al – 20Si after compression plasma flows impact, *Journal of the Belarusian State University. Physics*, Vol. **2**, pp., 25-33, 2021.

Tong, G., Dakui, L., Zuoshan, W., Xiangfa, L., Evolution, microhardness of ZrAlSi intermetallic and its impact on the elevated-temperature properties in Al–Si alloys, *Materials Science and Engineering*, Vol. **A 552**, pp. 523– 529, 2012.

Vilar, R., Conde, O., Franco, S., Crystallographic structure of Al_3Nb in laser-processed Al-Nb alloys, *Intermetallics*, Vol. **7**, pp. 1227-1233, 1999.

Wang, F., Qiu, D., Liu, Z., Taylor, J., Easton, M., Zhang, M., Crystallographic study of Al_3Zr and Al_3Nb as grain refiners for Al alloys, *Trans. Nonferrous Met. Soc. China*, Vol. **24**, pp. 2034−2040, 2014.

Zaguliaev, D.V., Konovalov, S.V., Ivanov, Yu.F., Gromov, V.E., Shlyarov, V.V., and Rubannikova, Yu.A., The effect of high-intensity electron beam on the crystal structure, phase composition, and properties of Al–Si alloys with different silicon content, *Prog. Phys. Met.*, Vol. **22**, no. 1, pp. 129-157, 2021.

Zhang, C., Lu, P., Xia, H., Yang, Z., Konovalov, S., Chen, X., Guan, Q., The microstructure and properties of nanostructured Cr-Al alloying layer fabricated by high-current pulsed electron beam., *Vacuum*, Vol. **167**, pp. 263–270, 2019.

Zhang, X., Huang, Y., Liu, Y., Xiao, Z., A comprehensive study of the $L1_2$-Al_3Nb/Al interface properties using first-principles calculations, *Journal of Materials Research and Technology*, Vol. **9**, no 6, pp. 12428–12442, 2020.

Zolotorevsky, V.S., Belov, N.A., Glazoff, M.V., *Casting aluminium alloys*. Elsevier, 2007.